ALIEN EARTHS

Which Nearby Planetary Systems Are Likely to Host Habitable Planets and Life?

MONTHLY NEWSLETTER

April 2026

Alien Earths is part of NASA's Nexus for Exoplanetary System Science program, which carries out coordinated research toward the goal of searching for and determining the frequency of habitable extrasolar planets with atmospheric biosignatures in the Solar neighborhood.

Our interdisciplinary teams include astrophysicists, planetary scientists, cosmochemists, material scientists, chemists, biologists, and physicists.

The Principal Investigator of Alien Earths is Daniel Apai (University of Arizona). The projects' lead institutions are The University of Arizona's Steward Observatory and Lunar and Planetary Laboratory.

For a complete list of publications, please visit the **AE Library** on the SAO/NASA Astrophysics Data System.

Recent Publications

Radiating Bondi Flows I: Dimensionless Framework and Constant Opacity Solutions

Radiating Bondi Flows II: Giant Planet Accretion Models

Analytical Estimates for Heliocentric Escape of Satellite Ejecta

Two Temperate Earth- and Neptune-sized Planets Orbiting Fully Convective M Dwarfs

Water Enrichment of Forming Sub-Netptune Envelopes Limited by Oxygen Exhaustion

Mantle Convection and Nightside Volcanism on Lava World K2-141b

Mangos – II. Five New Giant Planets Orbiting Low-mass Stars

NASA's Pandora SmallSat Mission: Simulated Modeling and Retrieval of Near-infrared Exoplanet Transmission Spectra

Radiating Bondi Flows I: Dimensionless Framework and Constant Opacity Solutions

Avery Bailey, Andrew Youdin, Kaitlin Kratter

Astro-ph: arXiv:2603.20373

In this paper, we extend the foundational work of Bondi (1952) to include the effects of radiative feedback in gas-pressure-dominated environments. We construct steady-state spherically symmetric accretion solutions including radiative heating and cooling. Under the simplifying assumption of a constant opacity, the solutions are controlled by four dimensionless parameters: the adiabatic index γ, optical depth through the Bondi radius τ_B, dimensionless luminosity at infinity $\tilde{L}_\infty$ and a characteristic dimensionless cooling time β. We present numerical solutions across the dimensionless parameter space $(\tau_B, \tilde{L}_\infty, \beta) \in [10^{-3}, 10^{3}]$ Contrary to radiation-pressure-dominated environments, radiative feedback primarily operates to suppress accretion -- particularly at high τ_B, $\tilde{L}_\infty$, and/or β. We also present analytic descriptions confirming the suppressive nature of this feedback and give the scalings for the accretion rate $\dot{M} \sim \tilde{L}_\infty^{-5/4}$ at large $\tilde{L}_\infty$, $\dot{M} \sim \tau_B^{-10/11}\, \beta^{-5/11}$ at large τ_B, and $\dot{M} \sim (\tilde{L}_\infty\, \tau_B)^{-5/8}$ for large $\tilde{L}_\infty\, \tau_B$. We discuss the potential role of convection in these steady-state solutions, and the particular relevance to problems of planet formation where radiative heating is significant, but the system remains in the gas-pressure-dominated regime.

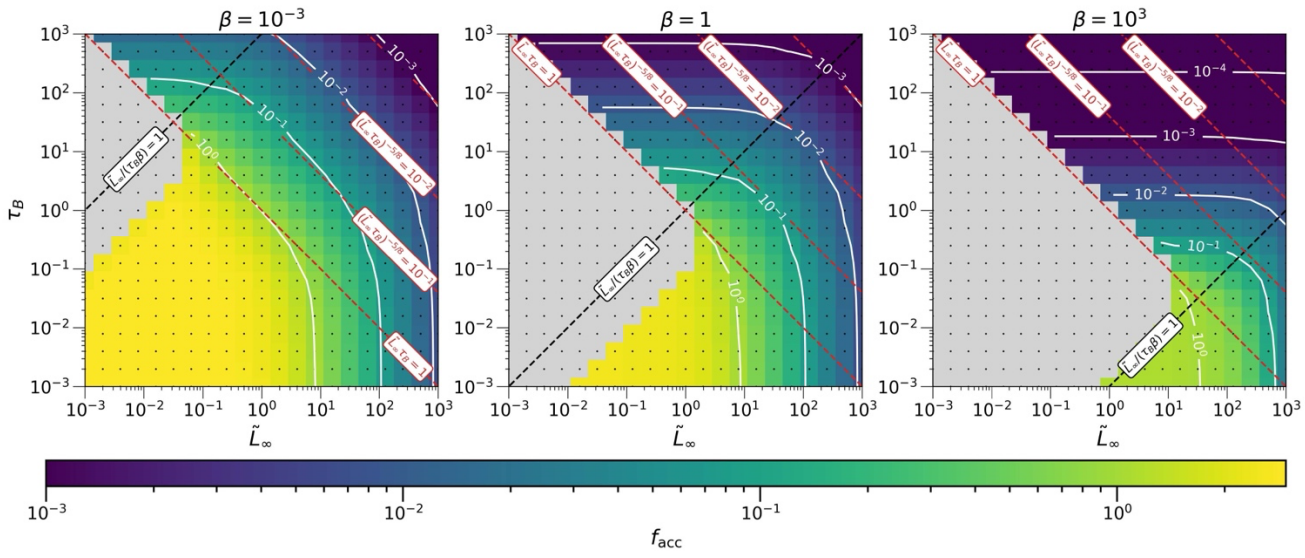

Figure 3. Slices at fixed $\beta \in (10^{-3}, 1, 10^{3})$ in the surveyed parameter space, mapping the steady-state accretion rates relative to the adiabatic Bondi rate. Each black dot corresponds to a computed steady-state solution on our model grid with the surrounding square colored according to the value of f_{acc}. Cells for which no transonic solution could be found are colored gray. Solid white contours are also drawn for each decade of f_{acc}. For reference, dashed lines for the conditions $\tilde{L}_\infty = \tau_B\beta$ and $f_{acc} = (\tilde{L}_\infty\tau_B)^{-5/8}$ with $f_{acc} = (10^{-3}, 10^{-2}, 10^{-1}, 1)$ are included (see Section 3.2 for the origin of these scalings).

Radiating Bondi Flows II: Giant Planet Accretion Models

Avery Bailey, Kaitlin Kratter, Andrew Youdin

Astro-ph: arXiv:2603.20377

In the core accretion model of giant planet formation, the late stages of runaway growth are regulated by the hydrodynamic infall of gas from the protoplanetary disk. For a subset of planet-disk pairings, this scenario is analogous to the classical Bondi problem, which has motivated a Bondi-like parameterization of accretion in some population synthesis models. Existing models and the associated classical Bondi rate however, are predicated upon an adiabatic equation of state. In reality, the planet and its associated accretion shock supply a luminosity that substantially heats the accretion flow. In Paper I of this series, we demonstrate that such radiative feedback can dramatically suppress accretion by orders of magnitude. Here we quantify this effect under realistic planet-forming conditions. We find that for planets forming in an unperturbed disk, accretion is suppressed by 1-2 orders of magnitude interior to ~10 AU. For planets that open a gap, this feedback is less dramatic and the effect is ~ 1 order in magnitude. We investigate the effect of various assumptions regarding dust opacities, shock efficiency, and planet radius and find this radiative suppression mechanism to be fairly insensitive to these effects. We also perform full time-dependent simulations demonstrating that the associated adverse entropy profiles are accurate and stable to convection. A simple and flexible set of open-source tools are provided to incorporate this radiative feedback into existing accretion models and population synthesis frameworks.

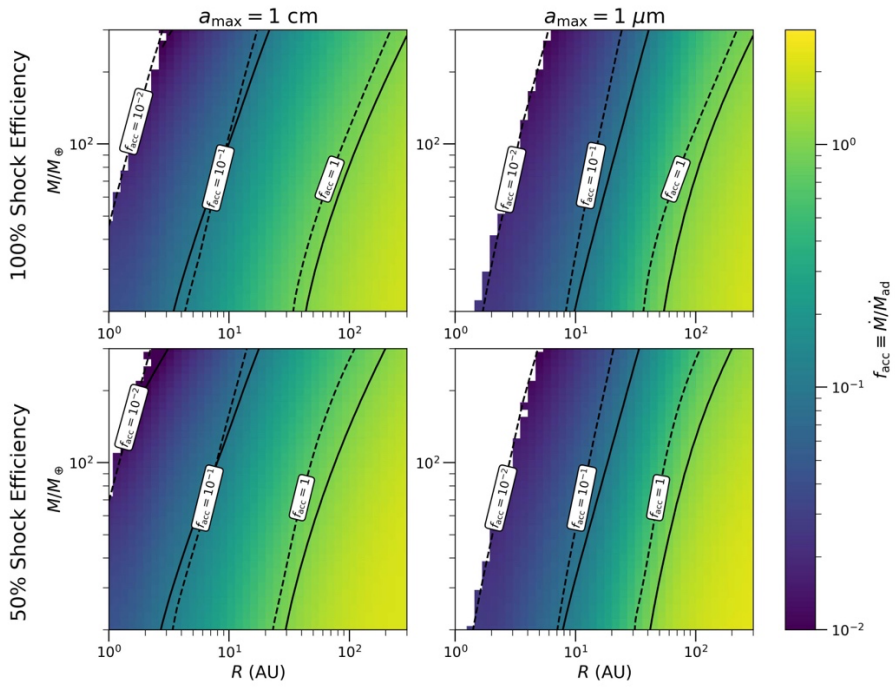

Figure 1. Steady-state accretion rates relative to the adiabatic Bondi rate as a function of planet mass and orbital distance.
Left column shows models with dust opacities that adopt a maximum particle size a_{max} = 1 cm. Right column shows models from the grid testing a different opacity by changing the maximum particle size to a_{max} = 10μm. Upper rows select models with a luminosity assuming all accretion energy is converted to radiation at a planetary boundary layer shock.
Lower rows assume this energy conversion is 50% efficient (or a doubling of shock radius which is degenerate with efficiency). Regions where the model grid of this work found no steady-state transonic accretion solution are left blank. Contours of f_{acc} are also overlaid at the [10_{-2}, 10_{-1}, 10_0] with solid lines. At the same levels, dashed contours estimating the accretion rates using the analytic formula (B7) from Paper I are shown for comparison.

Analytical Estimates for Heliocentric Escape of Satellite Ejecta

Jose Daniel Castro-Cisneros; Renu Malhotra; Aaron J. Rosengren

Icarus, Volume 445, e. 116845

We present a general analytic framework to assess whether impact ejecta launched from the surface of a satellite can escape the gravitational influence of the planet–satellite system and enter heliocentric orbit. Using a patched-conic approach and defining the transition to planetocentric space via the Hill sphere or sphere of influence, we derive thresholds for escape in terms of the satellite-to-planet mass ratio and the ratio of the satellite's orbital speed to its escape speed. We identify three dynamical regimes for ejecta based on residual speed and launch direction. We complement this analysis with the circular restricted three-body problem, deriving a necessary escape condition from the Jacobi integral at L_2 and showing that it is consistent with the patched-conic thresholds. Applying our model to the Earth–Moon system reveals that all three outcomes – bound, conditional, and unbound – are accessible within a narrow range of launch speeds. This behavior is not found in other planetary satellite systems, but may occur in some binary asteroids. The framework also shows that the Moon's tidal migration has not altered its propensity to produce escaping ejecta, reinforcing the plausibility of a lunar origin for some near-Earth asteroids.

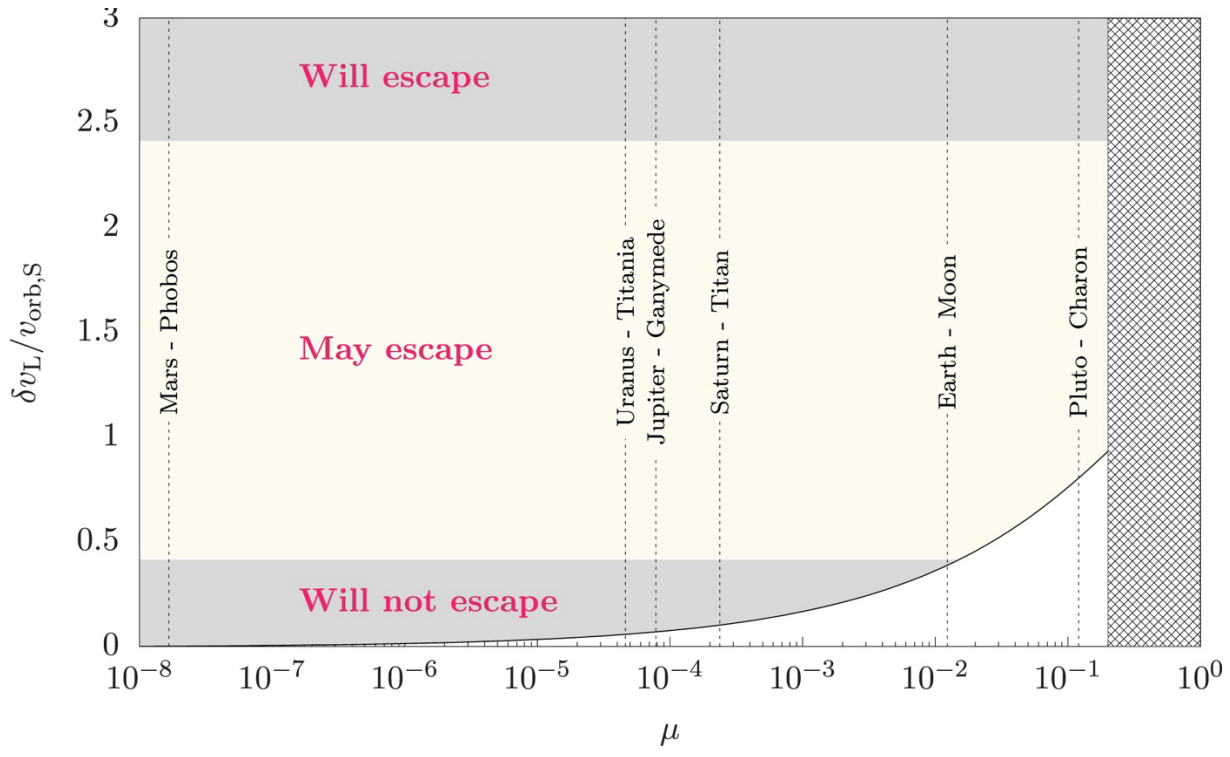

Figure 2. Ratio of residual speed at the satellite's Hill sphere and the satellite orbital speed, versus the satellite-to-planet mass ratio μ. The curve shows the bounding case of particles launched with speed equal to the satellite's escape velocity. Shaded regions represent the regions of different outcomes for ejecta launched above escape velocity. The stippled region is the range of $\mu > 0.2$ where the patched-conics approximation becomes less effective.

Two temperate Earth- and Neptune-sized planets orbiting fully convective M dwarfs

Madison G. Scott, Georgina Dransfield, Mathilde Timmermans, Amaury H.M.J. Triaud, Benjamin V. Rackham, Khalid Barkaoui, Adam J. Burgasser, Karen A. Collins, Michaël Gillon, Steve B. Howell, Alan M. Levine, Francisco J. Pozuelos, Keivan G. Stassun, Carl Ziegler, Yilen Gomez Maqueo Chew, Catherine A. Clark, Yasmin Davis,Tansu Daylan, Brice-Olivier Demory, Dax Feliz, Akihiko Fukui, Maximilian N. Günther, Emmanuël Jehin, Florian Lienhard, Andrew W. Mann, Clàudia Janó Muñoz, Norio Narita, Peter P. Pedersen, Richard P. Schwarz, Avi Shporer, Abderahmane Soubkiou, Sebastián Zúñiga-Fernández

Monthly Notices of the Royal Astronomical Society, Volume 547, Issue 1 March 2026

As the diversity of exoplanets continues to grow, it is important to revisit assumptions about habitability and classical HZ definitions. In this work, we introduce an expanded 'temperate' zone, defined by instellation fluxes between $0.1 < S/S_{\oplus} < 5$, thus encompassing a broader range of potentially habitable worlds. We also introduce the TEMPOS survey, which aims to produce a catalogue of precise radii for temperate planets orbiting M dwarfs with $T_{\rm eff} \leq 3400$ K. This work reports the discovery and characterization of two planets in this temperate regime orbiting mid-type M dwarfs: TOI-6716 b, a $R_{\rm b} = 0.98 \pm 0.07$ $R_{\oplus}$ planet orbiting its M4 host star ($R_{\star} = 0.231 \pm 0.015 R_{\odot}$, $M_{\star} = 0.223 \pm 0.011$ $M_{\odot}$, $T_{\rm eff} = 3110 \pm 80$ K) with a period $P = 4.7185898 \, ^{+0.0000054}_{-0.0000041}$ d , and TOI-7384 b, a $R_{\rm b} = 3.56 \pm 0.21$ $R_{\oplus}$ planet orbiting an M4 ($R_{\star} = 0.319 \pm 0.018 R_{\odot}$, $M_{\star} = 0.318 \pm 0.016$ $M_{\odot}$, $T_{\rm eff} = 3185 \pm 75$ K) star every $P = ^{+0.0000034}_{-0.0000036}$ d . The radii of TOI-6716 b and TOI7384 b have precisions of 6.8% and 5.9% respectively. We validate these planets with multi-band ground-based photometric observations, high-resolution imaging and statistical analyses. We find these planets to have instellation fluxes close to the inner (hotter) edge of the temperate zone, with $S_{\rm b} = 4.4 \pm 1.1$ $S_{\oplus}$ and $S_{\rm b} = 4.9 \pm 1.1$ $S_{\oplus}$ for TOI-6716 b and TOI-7384 b respectively. Also, with a predicted TSM similar to the TRAPPIST-1 planets, TOI-6716 b is likely to be a good rocky-world JWST target, should it have retained its atmosphere.

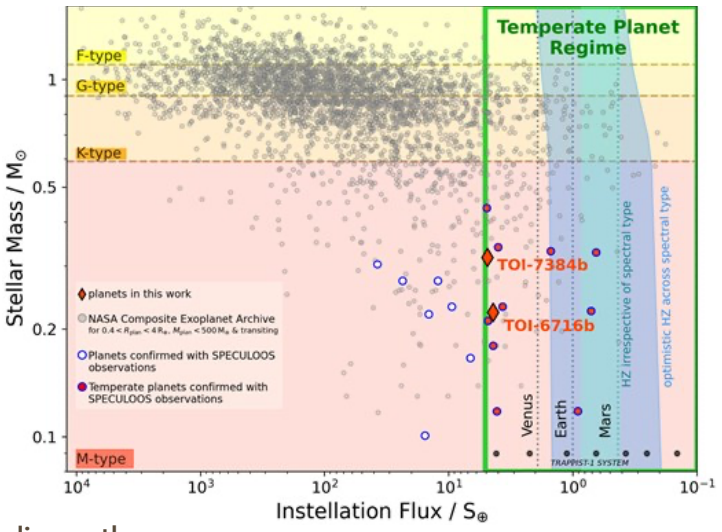

Figure 12. Stellar mass versus instellation flux for transiting planets with $0.4 < R_p < 4$ $R_{\oplus}$ and $M_p < 500$ $M_{\oplus}$ obtained from the Composite NASA exoplanet archive (small grey points). Instellation flux recalculated for all planets for consistency. Approximate spectral types are indicated by the shaded background and highlighted labels. Planets for which SPECULOOS observations contributed to the validation/confirmation are highlighted with blue circles TOI-6716b and TOI-7384n are depicted by red diamonds and sit at the inner (hotter) edge of the temperate regime (shown by the green box).

Water Enrichment of Forming Sub-Neptune Envelopes Limited by Oxygen Exhaustion

Tadahiro Kimura, Tim Lichtenberg

The Astrophysical Journal, Volume 1000, Number 2

The interaction between a magma ocean and a primordial atmosphere is increasingly recognized as a key process in shaping planetary envelope compositions. This coupling should strongly influence gas accretion, yet its role during the disk-embedded stage remains poorly constrained. We develop a time-dependent model that couples solid accretion, nebular gas accretion, and water enrichment and partitioning through magma–atmosphere interactions, along with post-disk thermal evolution and escape. We find that, for super-Earth-mass planets, water production is generally limited by the magma oxygen budget and typically ceases before disk dispersal. Subsequent nebular gas accretion dilutes the envelope toward hydrogen-dominated compositions, largely independent of the initial magma redox state. This establishes an upper bound on the envelope water fraction—the oxygen exhaustion limit—primarily set by the reactive oxygen inventory and the planet mass. After disk dispersal, degassing increases the water fraction only in Earth-mass planets undergoing strong escape, while super-Earths exhibit little change because surface pressures are hardly affected by escape. Magma–atmosphere coupling alone therefore cannot maintain water-rich envelopes in sub-Neptunes and produces a strong mass–composition relation imposed by the oxygen exhaustion limit. Highly enriched sub-Neptunes would therefore imply additional mechanisms such as late volatile delivery or post-disk giant impacts. The relation between planetary radius and envelope composition offers a means to infer magma properties, providing a pathway to connect present-day observables with early formation histories.

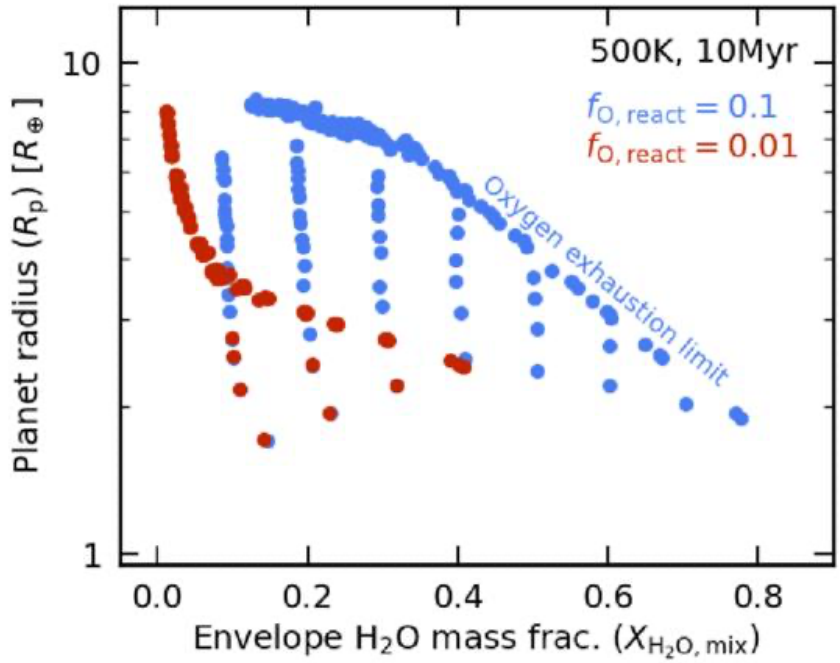

Figure 9. *Relation between planetary radius (*Rp*) and envelope water fraction ($X_{H2O,mix}$) at 10 Myr. Circles show simulations with various* M_{iso} *and* $X_{H2O,eq}$*. Blue and red points denote cases with* $f_{O,react}$ *= 0.1 and 0.01, respectively. Other parameters adopt the nominal values in Table 1.*

Mantle Convection and Nightside Volcanism on Lava World K2-141 b

Tobias G. Meier, Claire Marie Guimond, Raymond T. Pierrehumbert, Jayne Birkby, Richard D. Chatterjee, Chloe E. Fisher, Gregor J. Golabek, Mark Hammond, Thaddeus D. Komacek, Tim Lichtenberg, Alex McGinty, Erik Meier Valdés, Harrison Nicholls, Luke T. Parker, Rob J. Spaargaren, Paul J. Tackley

Monthly Notices of the Royal Astronomical Society, Volume 547, Issue 3, April 2026

Ultra-short period lava worlds offer a unique window into the coupled evolution of planetary interior and atmospheres under extreme irradiation. In this study, we investigate the mantle dynamics, nightside volcanism, and volatile outgassing on lava world K2-141 b ($1.54 R_\oplus$, $5.31 M_\oplus$) using two-dimensional convection models with tracer-based volatile tracking. Our simulations explore a range of interior configurations, including models with and without plastic yielding, basal versus mixed heating, core cooling, and melt intrusion. In models without plastic yielding (i.e. with a strong lithosphere), we find that mantle upwellings form at the substellar and antistellar points, while downwellings form near the day–night terminators at the boundary between the magma ocean and cold, solid nightside. These downwellings facilitate the recycling of crustal material, representing a form of asymmetric, single-lid tectonics. The resulting magma ocean thickness varies from 200 to 300 km depending on the model parameters, corresponding to about 2–3 per cent of the planet's radius. Continuous nightside volcanism produces a basaltic crust and gradually depletes the mantle of volatiles. We find that over a billion years, volcanic eruptions can outgas tens of bars of CO_2 and HO_2. We show that even relatively large volcanic eruptions on the nightside produce thermal emission signals of no more than 1 ppm, remaining below the current detectability threshold in thermal phase curves. However, for most models, outgassing rates are increased near the day–night terminators and future studies should assess whether such localized outgassing could lead to atmospheric signatures in transmission spectroscopy.

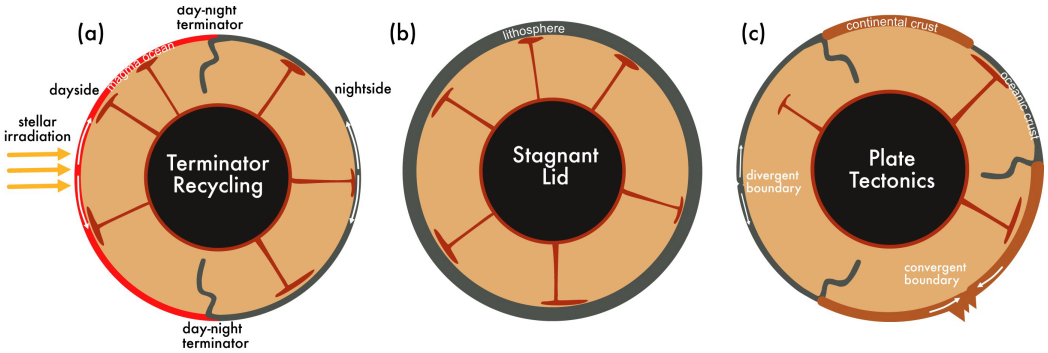

Figure 15.

Illustration of different tectonic regimes. (a) Terminator-recycling regime identified in this study, where downwellings form at the day–night terminator at the boundary between the magma ocean and cold, solid nightside. These downwellings enable the recycling of crustal material. (b) Stagnant-lid regime, characterized by a thick, immobile lithosphere. (c) Earth-like plate tectonics, where the lithosphere is divided into several rigid plates that move relative to each other, facilitating subduction zones and crustal recycling.

MANGOS — II. Five New Giant Planets Orbiting Low-mass Stars

G. Dransfield, M. Timmermans, D. Sebastian, B.V. Rackham, A. Burgasser, K. Barkaoui, A.H.M.J. Triaud, M. Gillon, J.M. Almenara, S.L. Casewell, K.A. Collins, A. Fukui, C. Janó Muñoz, S. Kanodia, N. Narita, E. Palle, M.G. Scott, A. Soubkiou, A. Stokholm, J. Audenaert, G.Á. Bakos, Y. Beletsky, Z.L. de Beurs, Z. Benkhaldoun, A. Burdanov, R.P. Butler, D. Caldwell, J.D. Crane, Y.T. Davis, B.O. Demory, E. Ducrot, Y. Gómez Maqueo Chew, M. Gachaoui, J.D. Hartman, M.J. Hooton, E. Jehin, S. Mercier, F. Murgas, C. Murray, P.P. Pedersen, F.J. Pozuelos, M. Rice, G. Ross, S.A. Shectman, E. Softich, M. Tala Pinto, A.M. Vandenburg, J. Villasenor, J. de Wit, S Zúñiga-Fernández

Monthly Notices of the Royal Astronomical Society, Volume 547, Issue 4, April 2026

Giant planets orbiting low-mass stars on short orbits present a conundrum, as in the most extreme cases their existence cannot be reconciled with current models of core accretion. Therefore, surveys dedicated to finding these rare planets have a key role to play by growing the sample to overcome small number statistics. In this work, we present MANGOS, a programme dedicated to the search for giant objects (planets, brown dwarfs, and low-mass stars) orbiting M dwarfs. We report on the discovery of five new giant planets (TOI-3288 Ab, TOI-4666 b, TOI-5007 b, TOI-5292 Ab, TOI-5916 b) first detected by *TESS* and confirmed using ground-based photometry and spectroscopy. The five planets have radii in the range of 0.99–1.12 R_{Jup}, masses between 0.49 and 1.69M_{Jup} , and orbital periods between 1.43 and 2.91 d. We reveal that TOI-3288 and TOI-5292 are wide binaries, and in the case of TOI-5292, we are able to characterize both stellar components. We demonstrate that the planets presented are suitable for further characterization of their obliquities and atmospheres. We detect a small but significant eccentricity for TOI-5007 b, although for this to be more robust, more observations are needed to fully sample the orbit. Finally, we reveal a correlation between stellar metallicity and planet bulk density for giant planets orbiting low-mass stars.

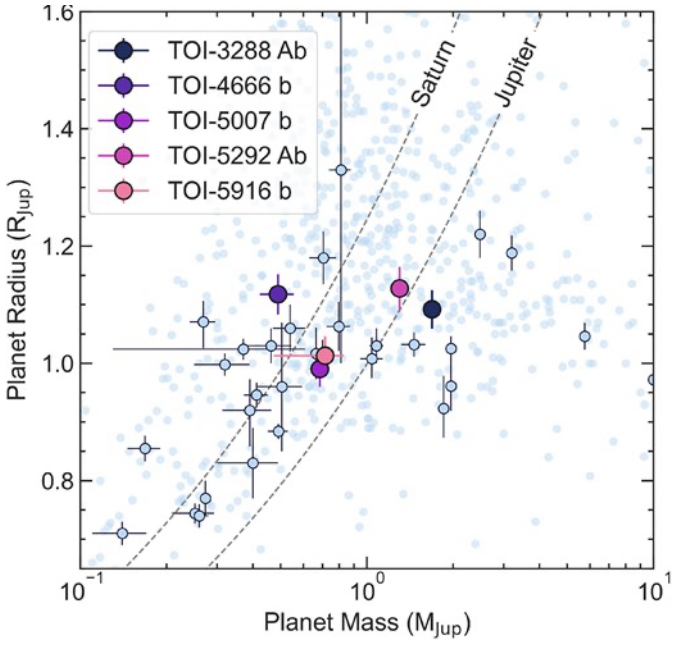

Figure 12.
Mass–radius of transiting giant exoplanets with measured masses, as queried from the NASA Exoplanet Archive. In the background in light blue are giant planets orbiting FGK stars. Light blue planets with black edges and error bars are MANGOS-type planets: giants orbiting M dwarfs with periods |$\lt 7$| d. The five planets presented in this work are shown in their respective colours. The two dashed lines show the density contours at Saturn and Jupiter's densities.

NASA's Pandora SmallSat Mission: Simulated Modeling and Retrieval of Near-infrared Exoplanet Transmission Spectra

Yoav Rotman, Peter McGill, Luis Welbanks, Benjamin V. Rackham, Aishwarya Iyer, Dániel Apai, Michael R. Line, Elisa V. Quintana, Jessie L. Dotson, Knicole D. Colón, Thomas Barclay, Christina Hedges, Jason F. Rowe, Emily A. Gilbert, Brett M. Morris, Jessie L. Christiansen, Trevor O. Foote, Aylin García Soto, Thomas P. Greene, Kelsey Hoffman, Benjamin J. Hord, Aurora Y. Kesseli, Veselin B. Kostov, Megan Weiner Mansfield, and Lindsey S. Wiser

The Astronomical Journal, Volume 171, Number 5

Pandora is a SmallSat mission dedicated to understanding exoplanets and their host stars by disentangling the impact of stellar heterogeneity on exoplanet transmission spectra. Selected as a NASA Astrophysics Pioneers mission in 2021, Pandora will provide simultaneous long-term visible photometric monitoring (0.4–0.7 μm) and low-resolution near-infrared (NIR) spectroscopy (0.9–1.6 μm) of transiting systems for the purposes of monitoring host star variability and characterizing exoplanetary atmospheres. Pandora's year-long prime mission from 2026 to 2027 coincides with the middle of a decade defined by targeted efforts for atmospheric characterization of exoplanets, offering a key opportunity to leverage this new resource to maximize science with JWST and other observatories. Here we investigate Pandora's anticipated performance for the general exoplanet population accessible to transit spectroscopy, from hot Jupiters to temperate sub-Neptunes. By modeling the atmospheres of five test cases broadly consistent with the bulk properties of HD 209458b, HD 189733b, WASP-80 b, HAT-P-18 b, and K2-18 b, we find that Pandora may provide abundance constraints as precise as ~1.0 dex for main atmospheric absorbers such as H_2O and CH_4. Then, we explore the synergies between Pandora and JWST. Our results suggest that targets with JWST data in the NIR can benefit from the addition of Pandora observations and result in more reliable abundance estimates than with JWST data alone. Moreover, Pandora can serve the community by providing precursory observations of targets of interest for JWST atmospheric characterization. We conclude by outlining strategies for the use of Pandora as a standalone observatory and in synergy with JWST.

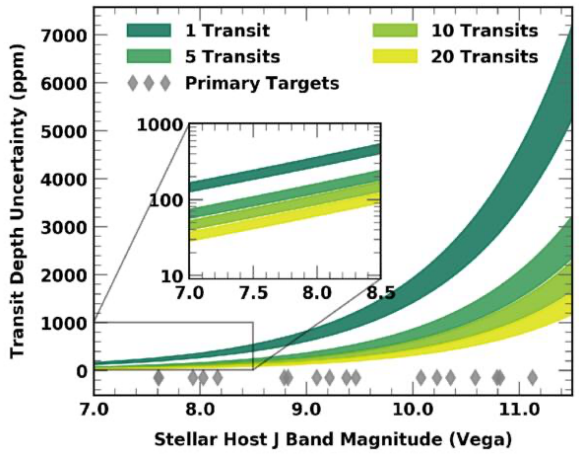

Figure 2. *The range of uncertainties predicted by our calculations for Pandora observations of a warm Jupiter-like system (here, WASP-80 b) with varying stellar magnitude, after binning to* $R \simeq 30$. *Different stellar fluxes and detector properties at different wavelengths will lead to different uncertainties throughout the bandpass; the bands here represent the range between the lowest and highest uncertainties. Stacking multiple observations will provide lower uncertainties, particularly for fainter targets. The inset shows the uncertainties for brighter stars, for which Pandora can achieve precisions as low as ~30 ppm when multiple transits are observed. The magnitudes of stars included in the Pandora primary target list are shown as diamonds.*